Tellus (1983), *35A*, 28–38

On the effect of model resolution on numerical simulation of blocking

By S. TIBALDI and L. R. JI*, *European Centre for Medium Range Weather Forecasts, Shinfield Park, Reading, Berks., England*

(Manuscript received February 12; in final form April 18, 1982)

ABSTRACT

A numerical case study of blocking is discussed briefly. The results indicate that model resolution seems to play a major role in the success of the simulation. It is argued that the effect of the initial conditions is somewhat less important than normally considered. The model used for all the experiments is the ECMWF spectral model.

1. Introduction

The horizontal scale of atmospheric blocking patterns is large and their dynamics has, with few exceptions (e.g. Green, 1977; Bengtsson, 1981), always been investigated in terms of planetary ultra-long waves. Therefore, in trying to numerically model this phenomenon, model resolution would perhaps be considered to be a non-critical modelling characteristic. If, however, as pointed out in different contexts by these authors, the interactions between smaller scale transient eddies and the quasi-stationary system are essential for the maintenance of the blocking pattern, the partial absence of such smaller eddies would strongly decrease the ability of a model to represent this phenomenon. A satisfactory representation of these eddies in terms of resolution would then become of fundamental importance. The purpose of this work is to report a numerical case study of blocking that showed a high degree of sensitivity to model resolution, so as to suggest that the scales of motion unresolved by the low resolution run but resolved by the high resolution run played a physically important role in the onset and maintenance of the blocking circulation.

The model used was the ECMWF spectral model (Baede et al., 1979) at the 2 triangular truncations T40 (low resolution) and T63 (high resolution). The scales of motion resolved explicitly by the T63 model but not by the T40 could be thought of as spanning the range between 300 and 500 km, expressing the concept of "scale" in terms of half wavelength. The parameterization of physical effects (radiation, condensation and effects of scales of motion beyond the model truncation, see Tiedtke et al. (1979)), was exactly the same in the 2 runs and reflects more or less the status of the "physics" of the ECMWF operational grid-point model as of August 1981.

2. The case study

The case selected took place during December 1978 and partially overlaps with the period covered by the JSC Working Group on Numerical Experimentation (WGNE) Case Study No. 1 (see JSC, (1981)), since we will discuss 10-day integrations starting from December 17, 1978 at 12 GMT. This development initiated the blocked-type circulation which characterized most of the winter period in 1978/79. The initial data used are taken from the ECMWF FGGE (First GARP Global Experiment) global initialized (non-linear normal mode initialization, see Williamson and Temperton, (1981)) analysis. Fig. 1 shows the 500 mb and 1000 mb height maps for the Northern Hemisphere for the initial data (day 0).

Figs. 2a to 5a show that, by day 5 of the integration period, a very large anticyclone had

* On leave from Institute of Atmospheric Physics, Academia Sinica, Beijing, China.

0280-6495/83/010028-11$2.50/0

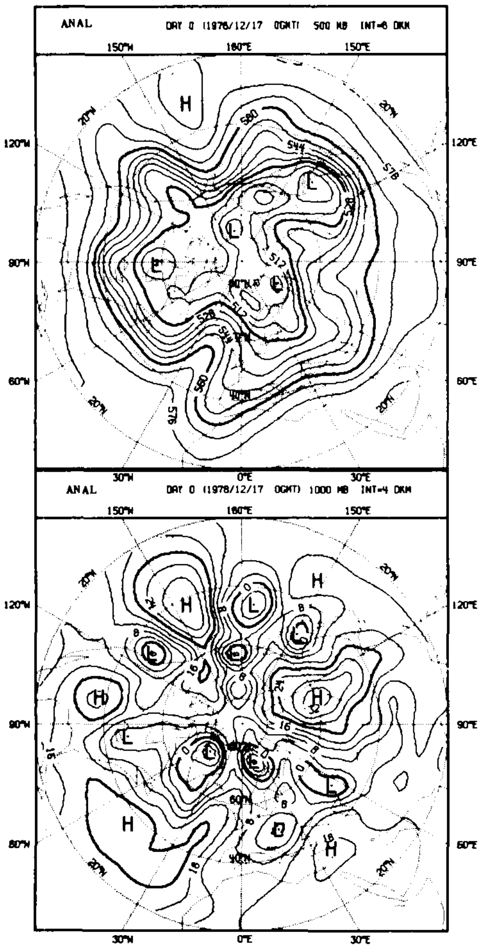

Fig. 1. FGGE analysis 00 GMT 17 Dec 1978; top, 500 mb geopotential height; bottom, 1000 mb geopotential height. Initial conditions used for the numerical experiments of different resolution. Intervals between isolines are, respectively, 8 dam (top, 500 mb) and 4 dam (bottom, 1000 mb).

established itself over the North Atlantic, diverting completely the flow of the westerlies. This large scale situation intensified at first and then was maintained, with little or no substantial change, for another week. By day 10 of the forecast period, the blocking pattern had invaded the whole of the Atlantic region, from 30° N to the North Pole (Fig. 5a).

Figs. 2 to 5 show the different synoptic behaviours that the 2 different resolution runs produced compared with the verifying FGGE analyses. Figures at the top, (a), show the verifying analysis; centre figures, (b), show the high resolution T63 run; figures at the bottom, (c), describe the low resolution T40 run. 500 mb height maps are to the left of the 1000 mb height maps. It is clear from the figures that the T63 forecast succeeds in capturing accurately most of the main features of the blocking event. The day 5 forecast correctly predicts the build-up of the blocking, down to several synoptic details of the flow; the amplitude is, however, underestimated. The day 8 forecast is characterized by a marked erroneous eastward displacement of the blocking feature. It, nevertheless, still shows a blocking pattern of realistic intensity with a very good representation of the split of the westerly jet at 500 mb. The day 10 forecast, although showing a much earlier weakening of the block, still contains some synoptic value. Note, for example, the realistic split of the block into a double structure, with 2 block-like patterns side by side, both at 500 and 1000 mb. On the other hand, the lower resolution run completely fails to accomplish the onset of the block, despite a very reasonable short range (e.g. day 3) forecast. By day 8, the 2 forecasts have completely diverged synoptically from each other, with the T40 run having erroneously drifted towards a much more zonal state.

It is interesting, at this point, to note that another low resolution run initiated from initial conditions of 12 h later (12 GMT 17 Dec 1978, experiment T40B) shows little improvement (see Fig. 6) in describing the development in the Atlantic, ending up by day 8 (actually day 7.5 for this experiment) with a block-like pattern in the wrong hemispheric quadrant. This would suggest that, in this particular case study, the model is as sensitive to the resolution as it is to the specification of the initial conditions, if not more so. It also shows, however, that the low resolution model is capable of producing blocks, since the one developed at day 7.5 of the T40B forecast (Fig. 6c) lasts up to the end of the 10 day integration (not shown).

Comparing the T63 and T40 objective scores (see Fig. 7), it can be noticed that the 2 experiments start diverging from each other only after day 4.5, except, of course, for the shorter waves upon which the impact of resolution is more immediate (day 1.5). After day 4, however, the main difference (to the advantage of the high resolution run) is to be found in the ultra-long wave components. For a more complete spectral

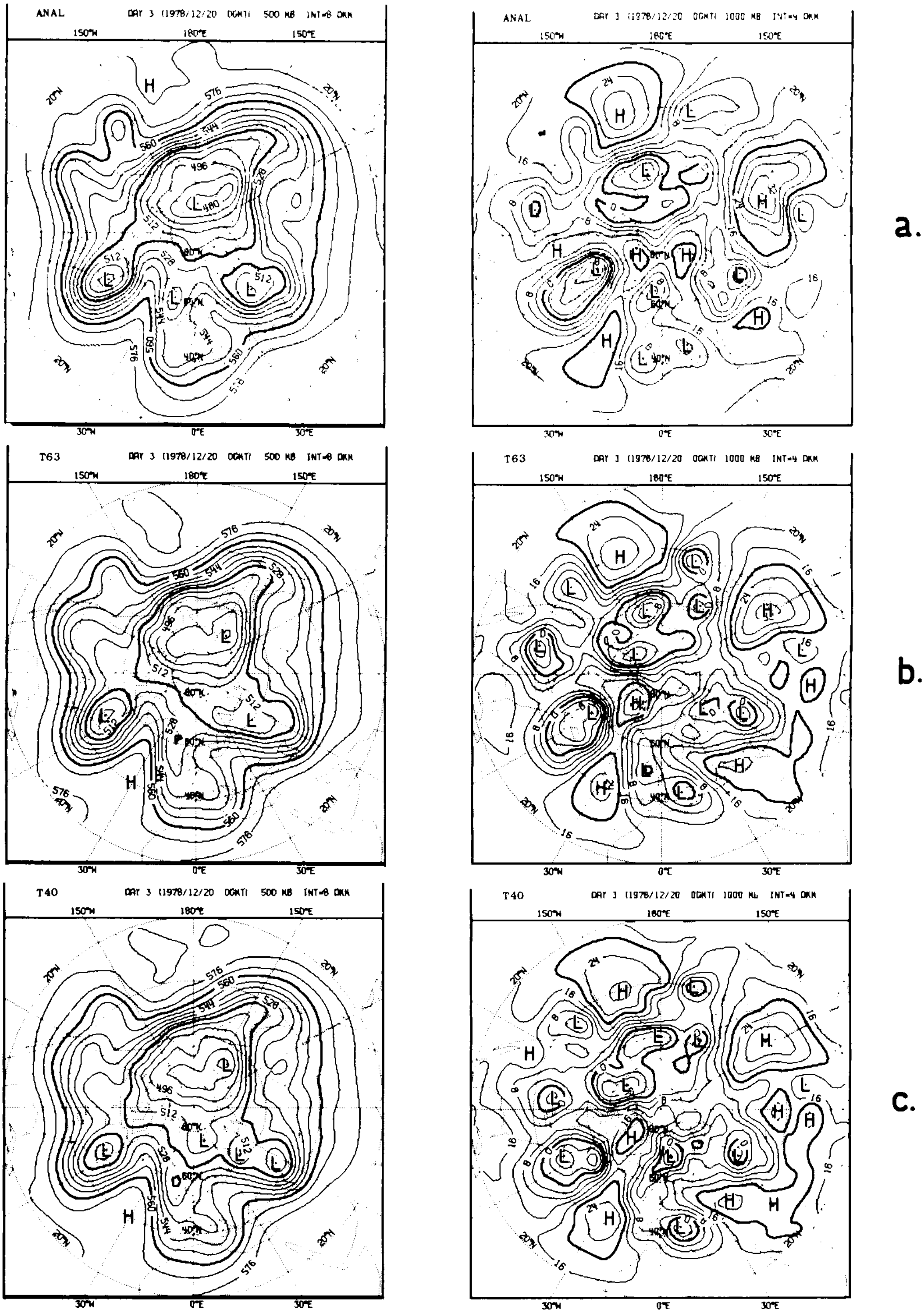

Fig. 2. Day 3 of the experiments. Top (a) is verifying analysis; centre (b) is the high resolution (T63) experiment; bottom (c) is the low resolution (T40) experiment. Left shows 500 mb geopotential height, right 1000 mb.

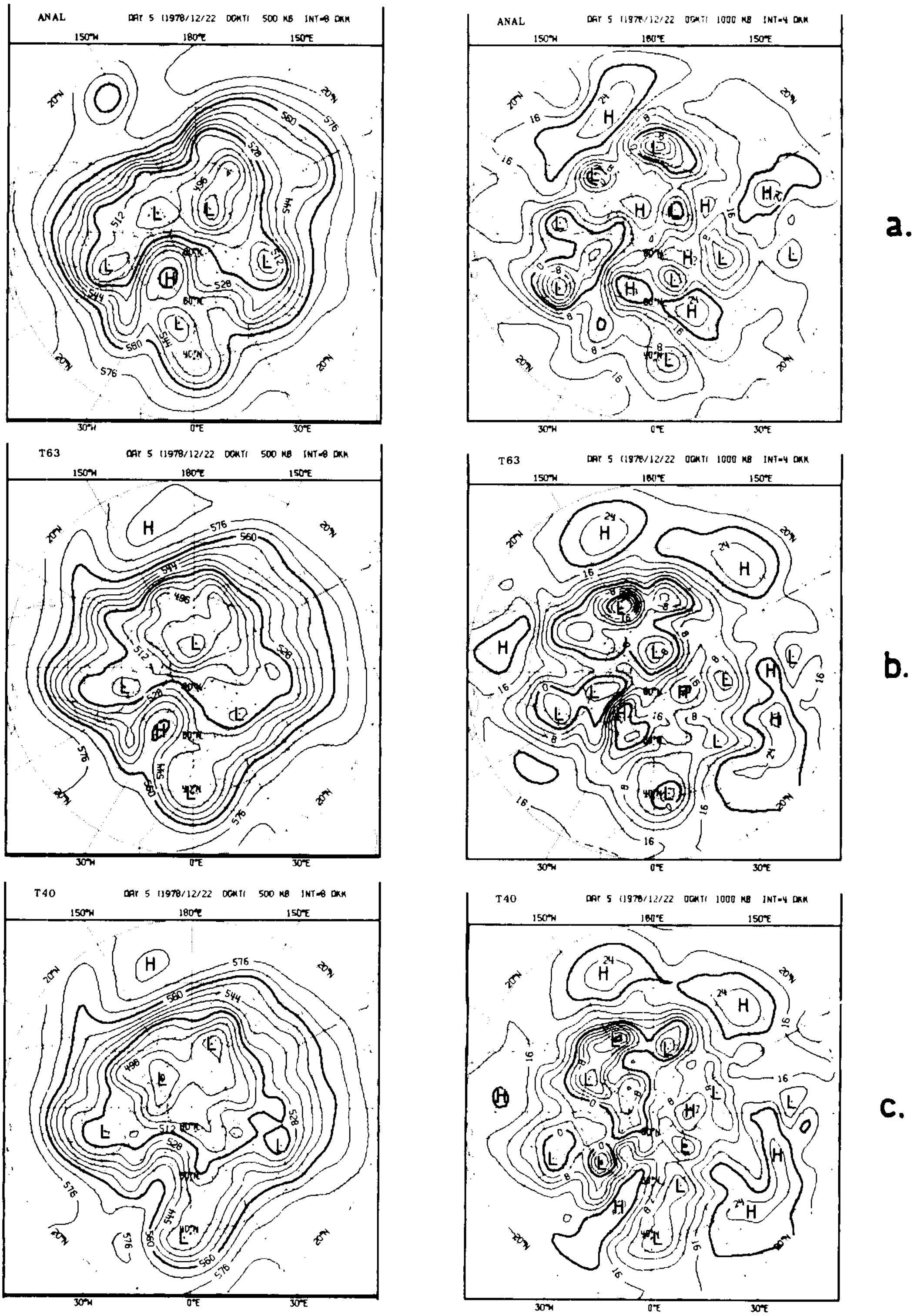

Fig. 3. As Fig. 2 but for day 5.

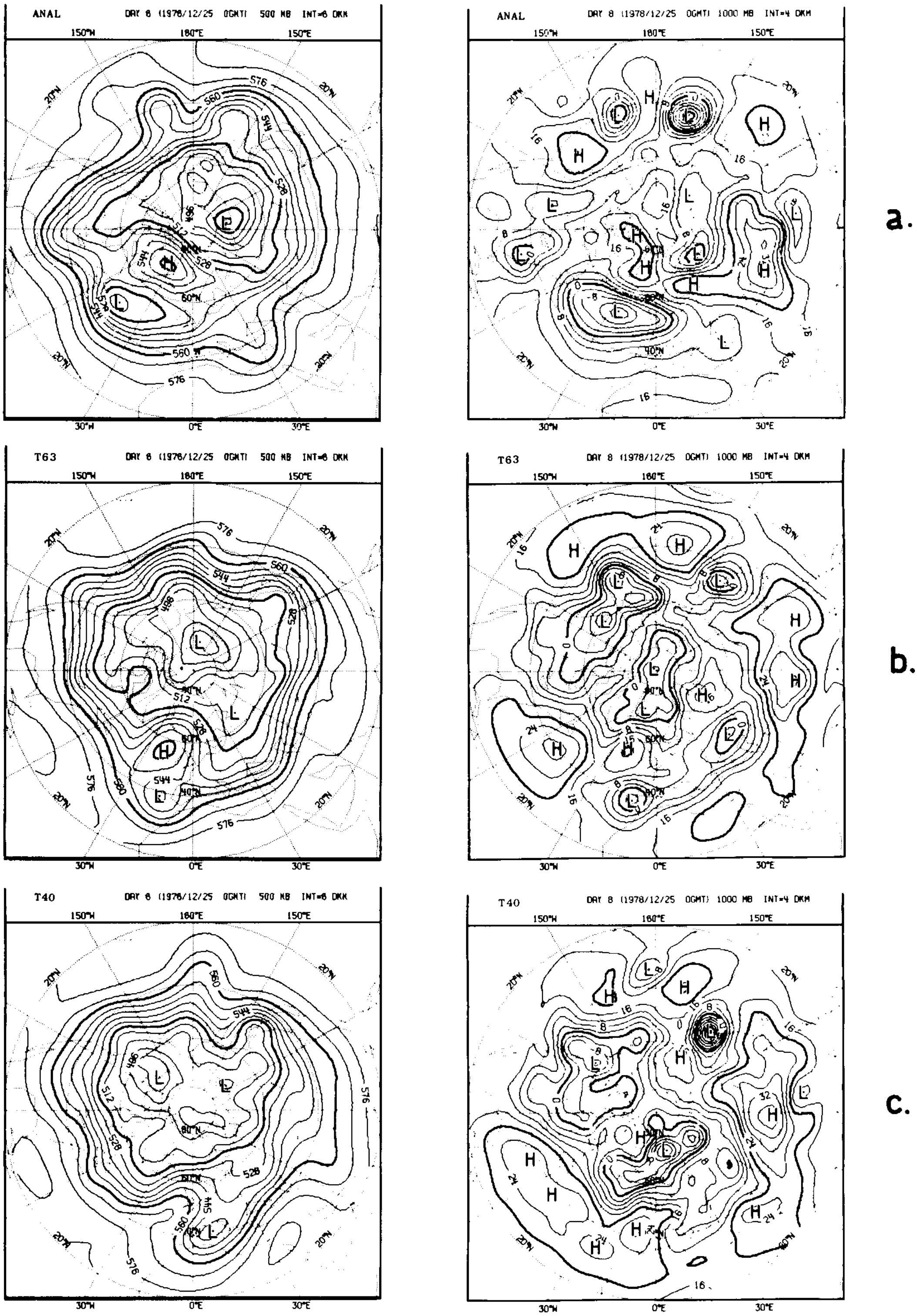

Fig. 4. As Fig. 2 but for day 8.

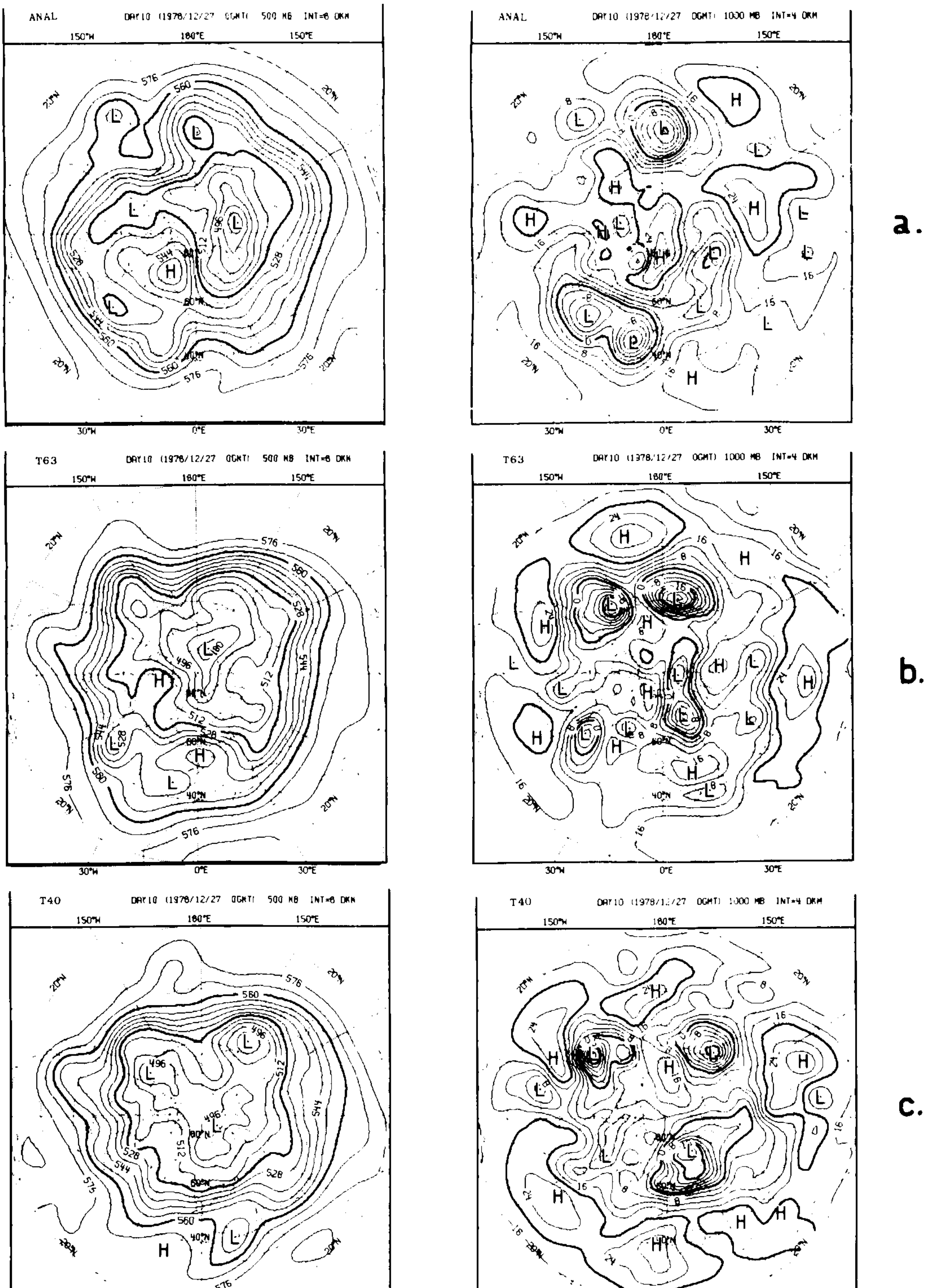

Fig. 5. As Fig. 2 but for day 10.

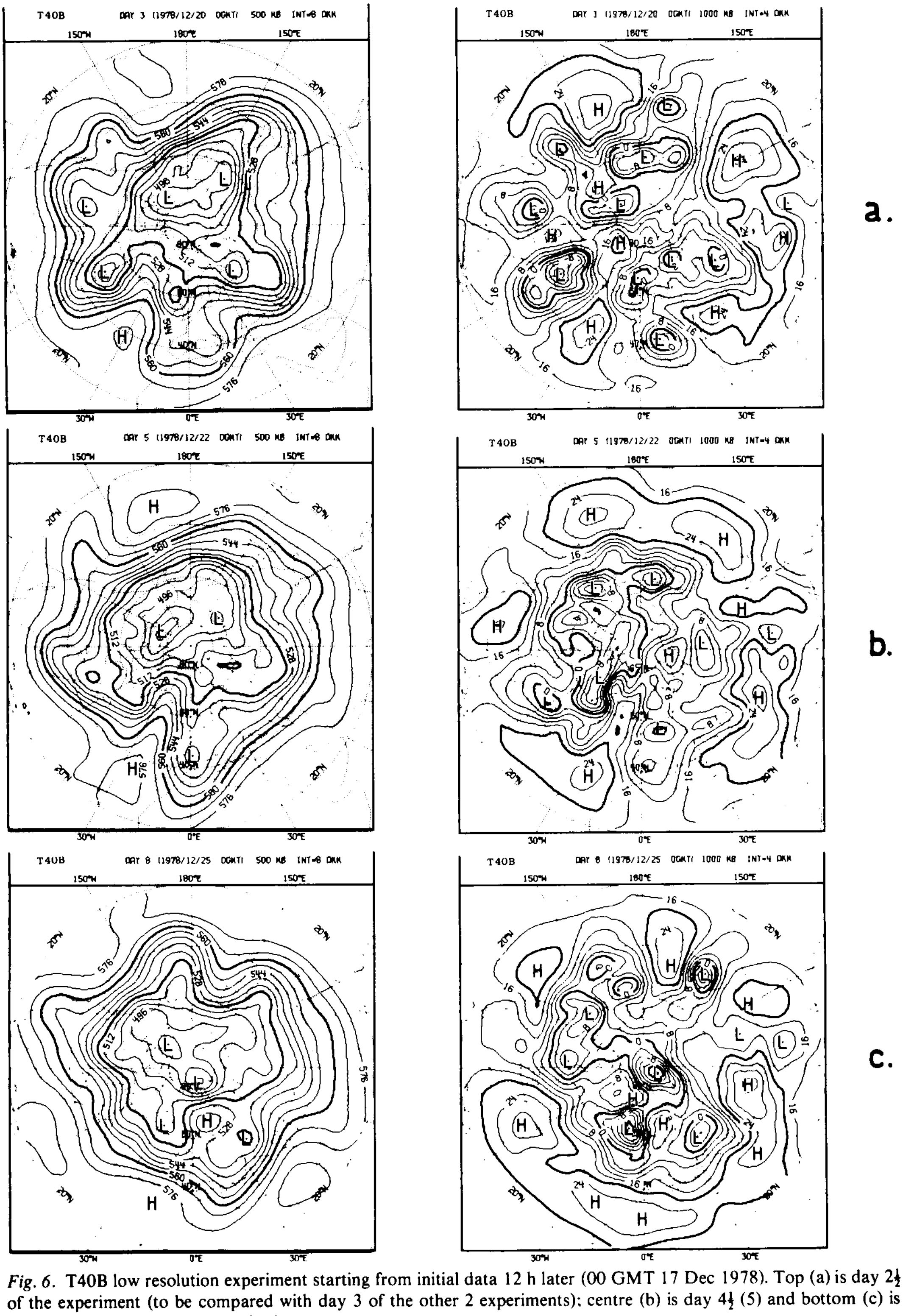

Fig. 6. T40B low resolution experiment starting from initial data 12 h later (00 GMT 17 Dec 1978). Top (a) is day $2\frac{1}{2}$ of the experiment (to be compared with day 3 of the other 2 experiments); centre (b) is day $4\frac{1}{2}$ (5) and bottom (c) is day $7\frac{1}{2}$ (8). Right and left as in Fig. 2.

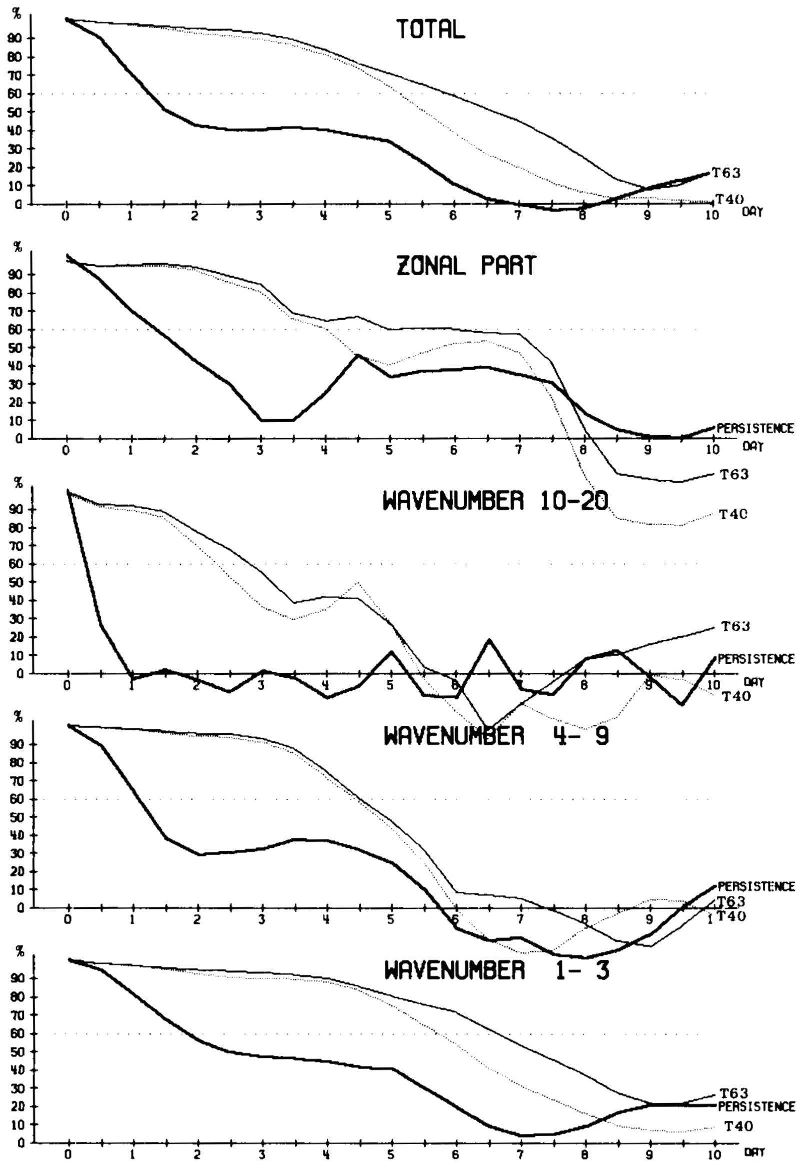

Fig. 7. Anomaly correlation of geopotential heights for the T63 and the T40 experiments as a function of time into the forecast. A spectral breakdown is shown, together with the total score. The correlation coefficient is computed between forecast anomaly fields and observed anomaly fields (climatology having been subtracted from both), from 20° to 82.5° N and from 1000 to 200 mb.

resolution comparison study of this type, the reader is referred to Jarraud et al. (1981).

The time evolution of the kinetic energy (Fig. 8) also shows that there is a sharp increase of KE in the wavenumber band 4 to 9 during the first 2 days of the integration, followed by a decrease taking place in parallel with a rapid growth of the KE in the wavenumber band 1 to 3. This might be interpreted in the following way. During a first stage (first 2 days) an intense development of a synoptic scale wave takes place which favours the onset of the block. Subsequently, an exchange of kinetic energy from medium (4 to 9) to long and ultra-long (1 to 3) waves takes place, thereby

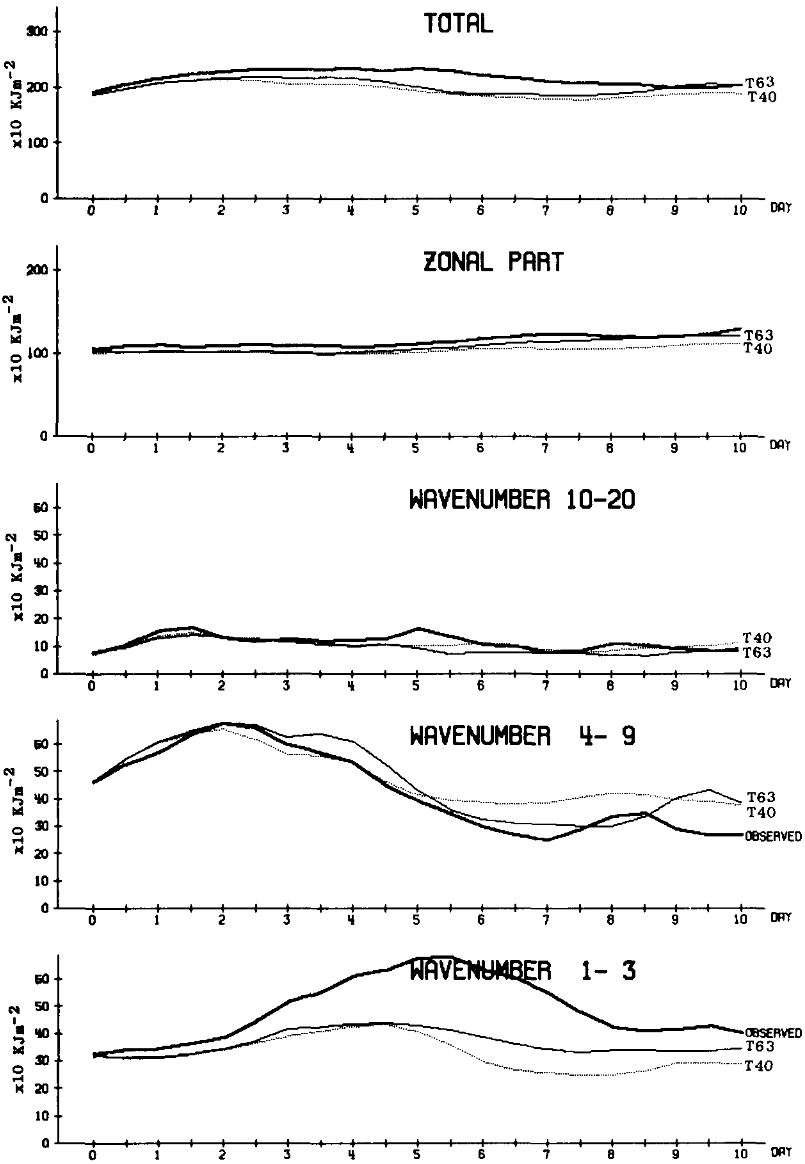

Fig. 8. Total kinetic energy as a function of time. Spectral breakdown and volume mean as for Fig. 7. The values are averages over the volume 20°–82.5° N and 1000–200 mb, and are expressed in tens of Joules per unit area (m^2).

maintaining the blocking situation. An adequate description of synoptic and subsynoptic scale waves (hence the sensitivity to resolution) would therefore be essential during both stages (see also Källén (1982) for a discussion of this point).

Fig. 9 shows the difference fields of 500 mb geopotential height between the T63 experiment and the T40 experiment days 2, 4, 6 and 8. It is possible here to see how the errors in the low resolution run originate from an underestimation of the develoment off the east coast of North America (Fig. 9a) and then grow to larger amplitudes. At day 4, a pronounced centre in the difference fields located on the North American continent, in the lee of the Rocky Mountains (Fig. 6b), suggests that the T40 run may not have given an adequate descrip-

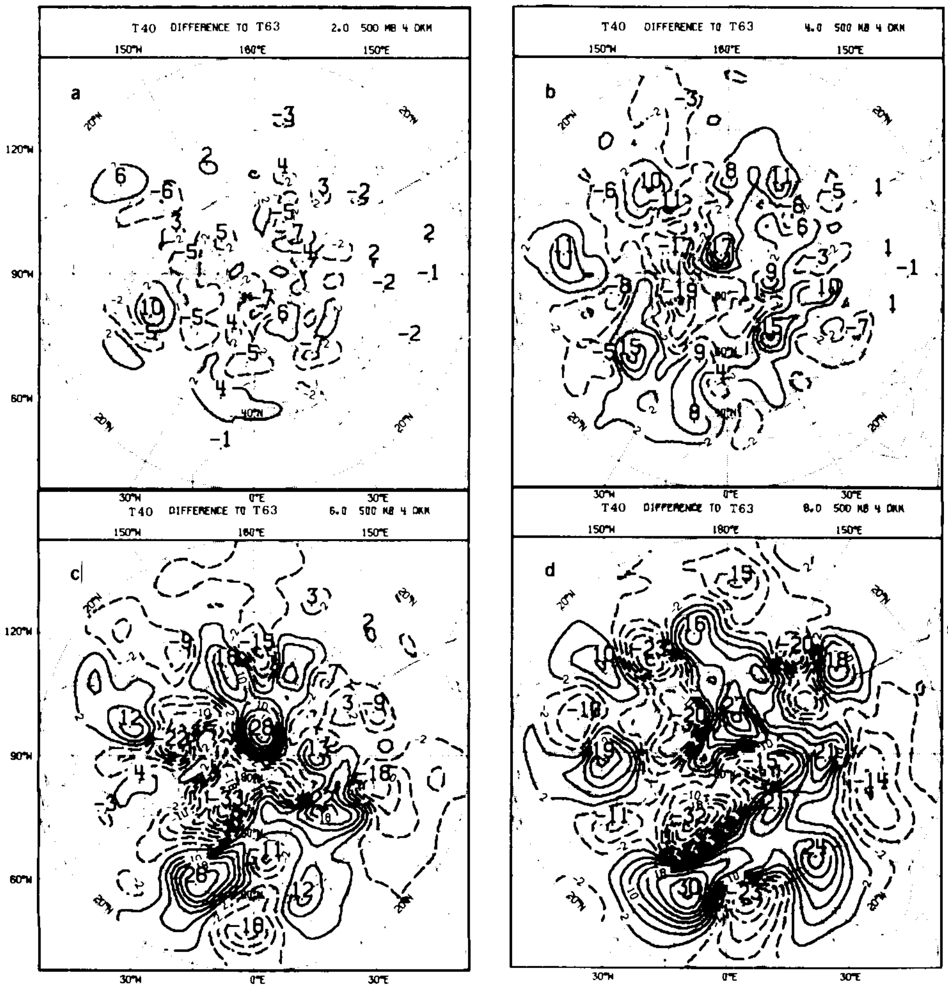

Fig. 9. Difference maps T63 runs minus T40 run: (a) day 2; (b) day 4; (c) day 6; (d) day 8. Only 500 mb geopotential height is shown.

tion of the mountain effects which cause successive downstream developments of troughs (Simmons and Hoskins, 1979). Such developments might, in turn, contribute to the onset and maintenance of the blocking (Kalnay-Rivas and Merkine, 1981).

3. Conclusions

The sensitivity to resolution that the ECMWF spectral model has shown in this Atlantic blocking case study indicates that the cumulative effects of scales of motion unresolved by a spectral triangular 40 truncation (but resolved by a T63 one) can have a crucial influence on the onset of such an important dynamical structure as blocking. These effects are most likely due to non-linear interactions between ultra-long waves and shorter waves and seem to affect the ability of the model to enter into a locally blocked state at the right time and in the right area. This confirms, on a particular blocking case study, general results previously obtained in a larger sample comparison (see Jarraud et al., 1981). This, of course, has an immediate bearing on the importance of model resolution in numerical weather prediction, mainly on time scales greater than 2 to 3 days.

This case study would also seem to lend more support to the view of blocking as a large scale circulation system supported vitally by comparatively smaller scale eddy disturbances, rather than purely as an "almost inescapable" state for both the real atmosphere and highly truncated models. These two points of view need not, however, be mutually incompatible (cf. Källén, 1982). When one moves from a highly truncated model to a realistic GCM (and, possibly, to the real atmosphere), the presence of smaller scale eddies (and of smaller scale forcings) could, on the one hand, substantially change the number and position of the possible quasi-steady states in the phase space of the system and the "attraction" properties of their attractor basins (cf. Wiin-Nielsen, 1979). Smaller eddies could also, on the other hand, contribute locally to the creation of conditions for the transition from one local quasi-steady state into another (Malguzzi and Speranza, 1981) and, moreover, contribute to the stability (and "steadiness") of a blocked-type state.

REFERENCES

Baede, A. P. M., Jarraud, M. and Cubasch, U. 1979. Adiabatic formulation and organisation of ECMWF's spectral model. *ECMWF Tech. Rep. No. 7*, 40 pp.

Bengtsson, L. 1981. Numerical prediction of atmospheric blocking. A case study. *Tellus 33*, 19–42.

Green, J. S. A. 1977. The weather during July 1976: some dynamical considerations of the drought. *Weather 32*, 120–126.

Kalnay-Rivas, E. and Merkine, L. O. 1981. A simple mechanism for blocking. *J. Atmos. Sci. 38*, 2077–2091.

Källén, E. 1982. Bifurcation properties of quasi-geostrophic, barotropic models and their relation to atmospheric blocking. *Tellus 34*, 255–265.

Jarraud, M., Girard, C. and Cubasch, U. 1981. Comparison of medium range forecasts made with models using spectral or finite-difference techniques in the horizontal. *ECMWF Tech. Rep. No. 23*, 96 pp.

JSC, 1981. Selection of FGGE cases for numerical experimentation. Report of the second session of the WMO/ICSU Joint Scientific Committee (JSC II), Annex G, Appendix C, WMO, Geneva.

Malguzzi, P. and Speranza, A. 1981. Local multiple equilibria and regional atmospheric blocking. *J. Atmos. Sci. 38*, 1939–1948.

Simmons, A. J. and Hoskins, B. J. 1979. The downstream and upstream development of unstable baroclinic waves. *J. Atmos. Sci. 36*, 1239–1254.

Tiedtke, M., Geleyn, J.-F., Hollingsworth, A. and Louis, J.-F. 1979. ECMWF model parameterization of sub-grid scale processes. *ECMWF Tech. Rep. No. 10*, 46 pp.

Wiin-Nielsen, A. 1979. On the asymptotic behaviour of a simple stochastic-dynamic system. *Geophys. Astrophys. Fluid Dyn. 12*, 295–311.

Williamson, D. L. and Temperton, C. 1981. Normal mode initialization for a multilevel grid-point model. Part II: Nonlinear aspects. *Mon. Wea. Rev. 109*, 744–751.